View metadata, citation and similar papers at core.ac.uk
brought to you by CORE
provided by Chalmers Publication Library

JTTEES 20:76–82
DOI: 10.1007/s11666-010-9543-7
1059-9630/$19.00 © ASM International

Peer Reviewed

Relationships Between Process Parameters, Microstructure, and Adhesion Strength of HVOF Sprayed IN718 Coatings

Christophe Lyphout, Per Nylén, and Lars Östergren

(Submitted May 7, 2010; in revised form July 30, 2010)

Fundamental understanding of relationships between process parameters, particle in-flight characteristics, and adhesion strength of HVOF sprayed coatings is important to achieve the high coating adhesion that is needed in aeronautic repair applications. In this study, statistical Design of Experiments (DoE) was used to identify the most important process parameters that influence adhesion strength of IN718 coatings sprayed on IN718 substrates. Special attention was given to the parameters combustion ratio, total gas mass flow, stand-off distance and external cooling, since these parameters were assumed to have a significant influence on particle temperature and velocity. Relationships between these parameters and coating microstructure were evaluated to fundamentally understand the relationships between process parameters and adhesion strength.

Keywords adhesion strength, Design of Experiments, HVOF, Inconel 718 coating, microstructure

1. Introduction

Coating adhesion is one of the most important properties of thermally sprayed coating systems since it controls the coating's lifetime and its applicability (Ref 1). The adhesion is dependent on several factors such as pretreatment, process conditions during spraying and posttreatment (Ref 2, 3). In order to fundamentally understand the relationships between process parameters and the coating adhesion strength, establishment of relationships between controllable process parameters, in-flight properties of the injected powder (particles velocity and temperature), and microstructure properties is important. To be able to quantify the relationships, a measurement method for high adhesion strength is necessary. Such a method was developed in previous work since the standard tensile test ASTM C633-79 (Ref 4) which is conventionally used to measure coating adhesion strength, is limited by the strength of the polymer-based adhesive. The microstructure properties, porosity and oxides content are also difficult to determine in HVOF coatings by industrial standardized methods due to the low porosity and oxide levels in this process, why specific image analysis algorithms had to be developed. In this work, Design of Experiments (DoE) was used to establish relationships between process parameters, particle in-flight diagnostic, microstructure properties, and coating adhesion strength. DoE is a standard statistical approach conventionally used to study relationships between process parameters and coating microstructure in thermal spray. The approach is usually a stepwise procedure starting with screening fractional or full factorial designs to response surface designs for optimization purposes. In this study, a full factorial design was selected since this design can gain valuable insight in how different process parameters interact on several responses such as microstructure features and coating adhesion strength. It should be noted that quantification or discretization of all factors and responses is necessary when using DoE and that the results are dependent on the selected levels of the factors. Combustion ratio, total mass flow, stand-off distance (SOD), and external cooling were in this study selected as factors. Particle velocity, particle temperature, coating porosity, oxides content, and adhesion strength were selected as responses.

2. Experimental Procedure

2.1 Spraying Process

Inconel 718 powder was deposited on Inconel 718 substrates using a Sulzer-Metco HVOF hybrid DJ-2600 gun, assisted with an automatic external air cooling

This article is an invited paper selected from presentations at the 2010 International Thermal Spray Conference and has been expanded from the original presentation. It is simultaneously published in *Thermal Spray: Global Solutions for Future Applications, Proceedings of the 2010 International Thermal Spray Conference*, Singapore, May 3-5, 2010, Basil R. Marple, Arvind Agarwal, Margaret M. Hyland, Yuk-Chiu Lau, Chang-Jiu Li, Rogerio S. Lima, and Ghislain Montavon, Ed., ASM International, Materials Park, OH, 2011.

Christophe Lyphout and **Per Nylén**, University West, Trollhättan, Sweden; and **Lars Östergren**, Volvo Aero Corporation, Trollhättan, Sweden. Contact e-mail: christophe.lyphout@hv.se.

Table 1 Design matrix of spray conditions

Run name	Run order	Combustion ratio	Mass flow[a]	SOD[a]	External cooling
N6	1	0.5	1	−1	Yes
N3	2	0.5	−1	1	No
N4	3	0.5	1	1	No
N7	4	0.5	−1	1	Yes
N10	5	0.5	0	0	Yes
N9	6	0.5	0	0	Yes
N11	7	0.5	0	0	Yes
N1	8	0.5	−1	−1	No
N8	9	0.5	1	1	Yes
N5	10	0.5	−1	0	Yes
N2	11	0.5	1	0	No
N12	12	0.5	0	0	Yes
N13	13	0.7	1	0	Yes
N14	14	0.3	−1	0	Yes

[a]*1* high, *0* medium, *−1* low

system. Oxygen/hydrogen gases were chosen as the oxy-fuel mixture (Table 1). Substrate material of Inconel 718 coupons with 6.4 mm thickness and 25.4 mm in diameter were sprayed up to 500-μm thickness with an Inconel 718 powder feedstock material (AMDRY1718) with identical composition as the substrate material. Prior to spraying, substrates were degreased and automatically grit blasted to a mean roughness (Ra) of 2.5 μm. Sets of 10 samples were prepared for each experimental run.

2.2 Statistical Model

The investigation was performed using the statistical software MODDE© (MODeling of DEsign), MKS Umetrics AB, Sweden. The full factorial design consisted of 11 experimental runs, including three center point runs N9, N10, and N11 (Table 1). The runs were performed in a random order to increase model reliability. Multiple linear regression (MLR) was used to establish the relationships between the factors and the responses. The models were used both for investigation and prediction purposes. A separate MLR model was derived for each response variable to establish a best fit. A set of three additional runs were finally added in which the oxygen to fuel ratio were varied, keeping a constant total gas flow in all three runs. These three runs were not included in the model building. They were only used to investigate if particle temperature and velocity could be more extensively varied, thus enabling establishment of qualitative relationships between particle in-flight parameters and coating adhesion strength.

2.3 On-line Diagnostics

The DPV2000 (Tecnar Ltd. St-Bruno, QC, Canada) system was used to monitor particle in-flight properties characteristics for all spray conditions. The velocity is in this system determined by a time-of-flight method corresponding to measurement of the transit time between two optical slits. Particle temperature is determined by two-color pyrometry. Approximately 2000 particles were sampled for each condition, and used for calculation of average velocity and temperature. The measurements were performed at the stand-off spray distance (SOD). It should be noted that even if the spray parameters were identical, particles that build up the coatings and particles that are scanned by the DPV system cannot be considered as part of the same statistical population.

2.4 Coating Microstructure

HVOF coating microstructure is known to contain low amount of oxides typically formed at the periphery of particles prior to successive impacts. High compaction due to the high kinetic energy of the impinging particles results in low porosity values compared to other thermal spray processes. The standard ASTM E562 (Ref 5) procedure was for this reason not applicable in this study. Image analyses were instead used to determine porosity and oxide contents. Image processing and analysis algorithms were developed using the ADCIS Aphelion™ software. Calibration of the procedure was made by using the ASTM E562 point count standard (Fig. 1b) on a reference coating in order to determine appropriate threshold functions from the original frequency histogram (Fig. 1c), to be able to dissociate pores (Fig. 1d) from oxides (Fig. 1e). A significant decrease in the standard deviations for both porosity and oxides values were obtained thus enabling distinction between sets of samples (Fig. 1f).

2.5 Adhesion Strength Characterization

In order to overcome the limitation in adhesion strength in the standard ASTM C633-79 tensile test (Ref 4), an alternative method had to be developed. The polymer-based adhesive FM-1000 was substituted by a silver-based filler material. Induction heating was used in this method to melt the filler material, which was shaped into pre-forms to fit the diameter of the counter part sections (Fig. 2). The maximal tensile adhesion strength of the braze material was in earlier work optimized to 300 MPa (Ref 6), which is enough to quantify the tensile adhesion strength of HVOF sprayed coatings. In the present investigation, all failures were located at the coating/substrate interface which confirmed the applicability of the developed method.

3. Results and Discussion

3.1 Relationships Between Process Parameters and Adhesion Strength

The relationships between process parameters, i.e., total mass flow, spray distance and external cooling level, and particle in-flight properties and adhesion strength could be well described by MLR models (Table 2). The coefficients of linear regression (R2) have to be considered as very high for both particles velocity and temperature. Examples of main effect plots for the selected responses are shown in Fig. 3, when the total mass flow varies from its low to high level whereas spray distance

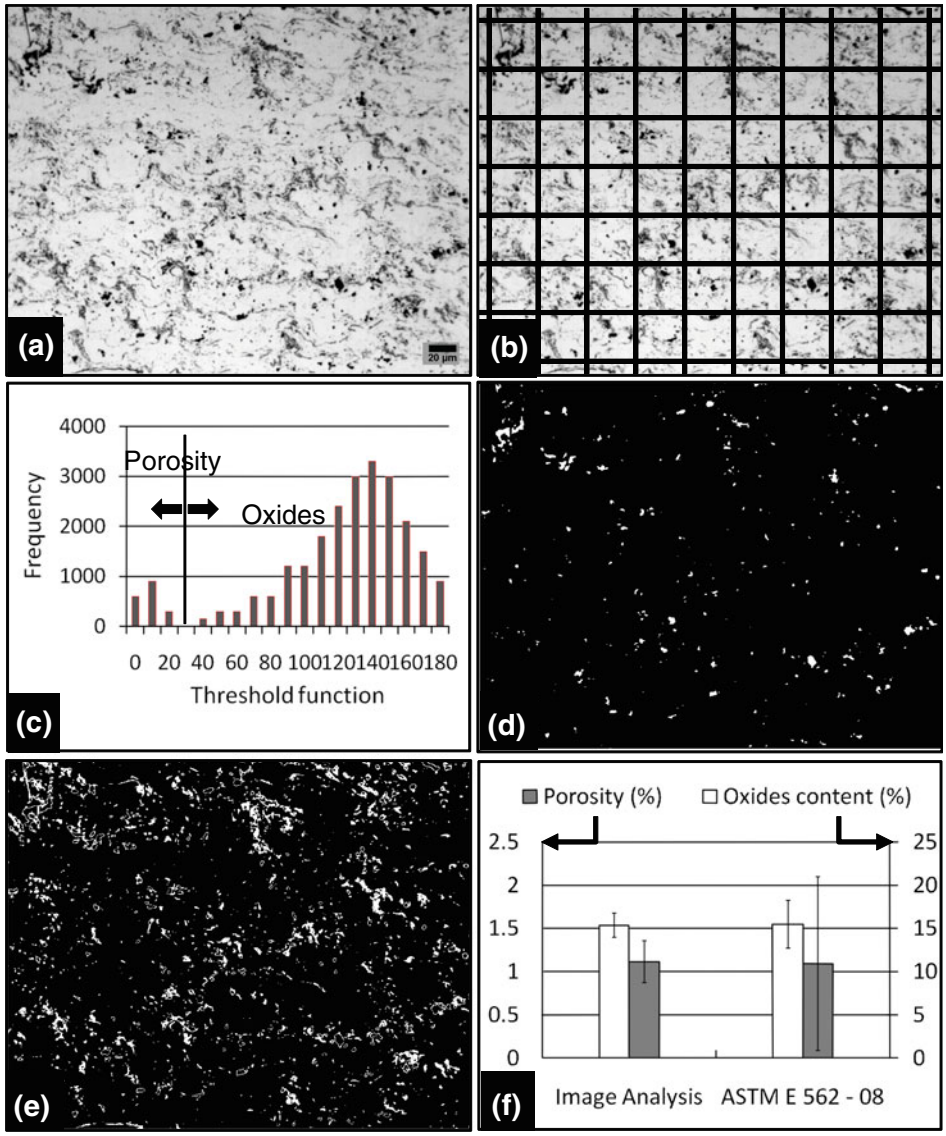

Fig. 1 Optical microscopy (200×) of standard reference (a), calibration using ASTM E562 point count procedure (b), frequency histogram (c) of the original image to dissociate porosity (d) from oxides content (e), and standard deviations for both methods (f)

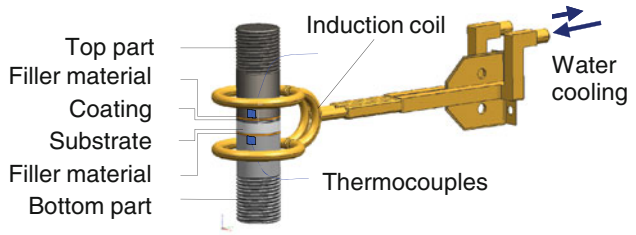

Fig. 2 Schematic of the induction brazing system used for adhesion strength tensile tests

and cooling parameters in the design were held constant at their averages. The error bars in the figures correspond to a confidence level of 0.95. An increase of the total mass flow significantly increases the particle velocity (Fig. 3b),

Table 2 Statistics from MLR regression models for process parameters map

Coeff.	Adhesion strength	Particle temperature	Particle velocity
Runs	11	11	11
DF	6	6	6
R2	0.811	0.944	0.975
Q2	0.307	0.901	0.959
RSD	13.41	3.361	7.034
Conf.lev.	0.95	0.95	0.95

DF residual degree of freedom, *R2* coeff. linear regression, *Q2* coeff. prediction ability, *RSD* residual standard deviation

whereas the particle surface temperature remains fairly constant (Fig. 3c). The effect of substrate cooling on adhesion strength is presented in the countour prediction

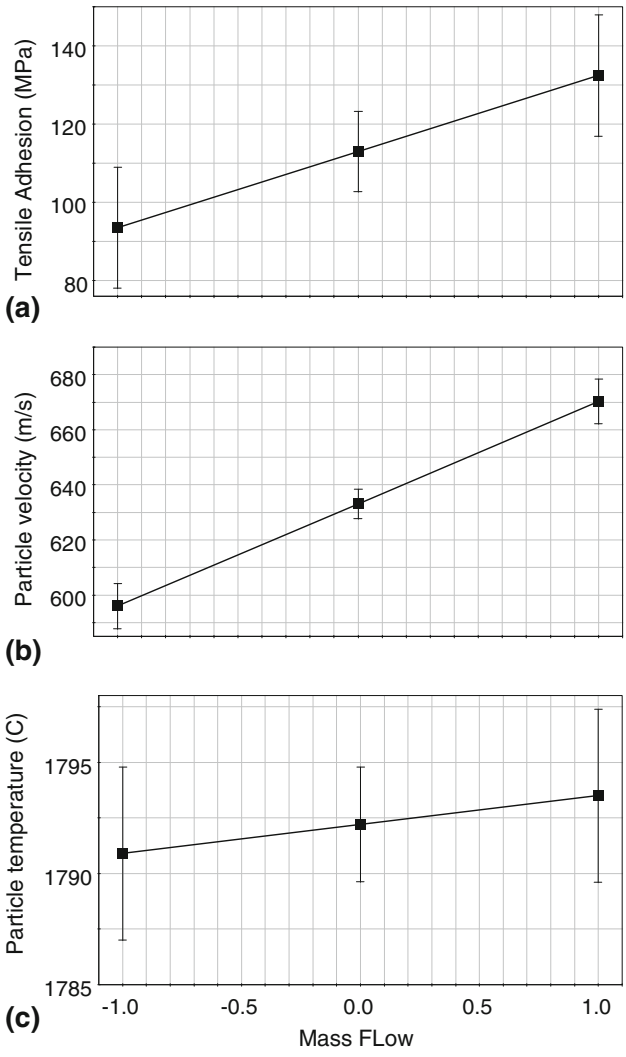

Fig. 3 Main effect plots for adhesion strength (a), particle velocity (b), and particle temperature (c)

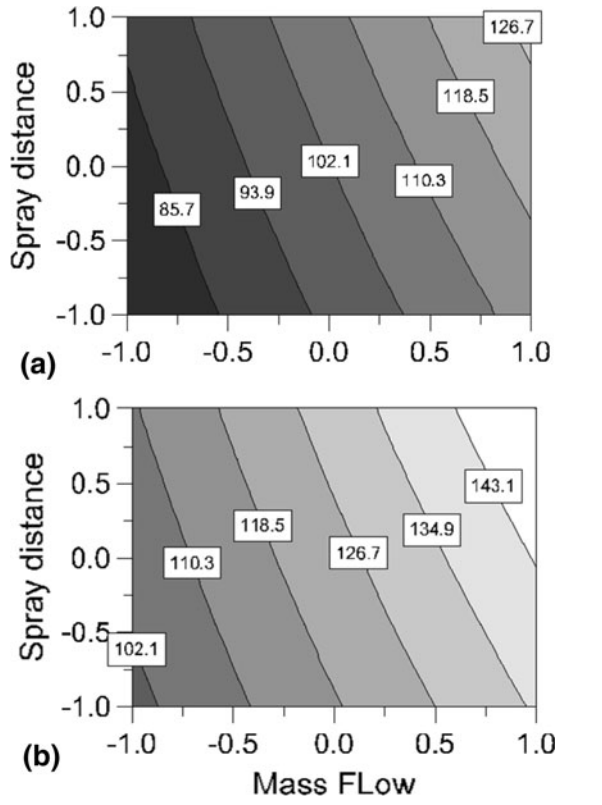

Fig. 4 Contour plots of coating adhesion strength (MPa) with (a) and without (b) substrate cooling

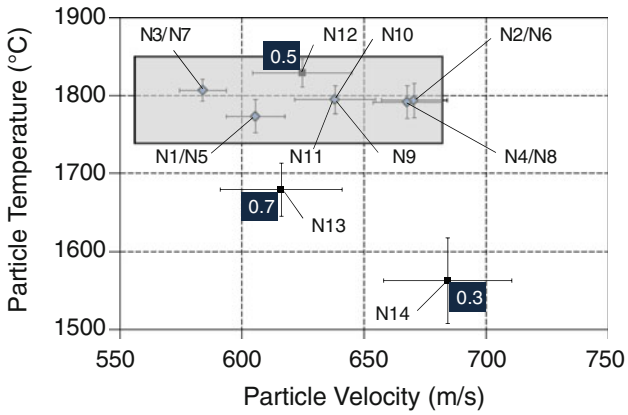

Fig. 5 Particle in-flight property process map for the different experimental runs

plots in Fig. 4. The external cooling has a substantial effect on coating adhesion strength. Under identical spraying parameters, no cooling results in 25% increase in adhesion strength.

3.2 Relationships Between Particle In-flight Properties and Adhesion Strength

Significantly higher particle velocities were measured in the even runs N2-N4-N6-N8 compared to the odd-runs ones N1-N3-N5-N7 (Fig. 5). This can be explained by the increase of the total mass transfer under a constant stoichiometric combustion ratio (of 0.5), which increases the kinetic energy of in-flight particles, without influencing their thermal energy which were almost constant in the different spray runs. To be able to study the relationships between particle in-flight temperature and adhesion strength, three new runs were added (Table 1). Significantly lower particle temperatures were obtained with an oxidizing (N13) and reducing flame (N14), while processing a constant total gas flow rate (Fig. 5). Keeping a fairly constant particle temperature and increasing the particle velocity gives a significantly higher coating adhesion strength (Fig. 6). Keeping a high particle velocity and increasing the particle temperature increases the adhesion strength (Fig. 6). The overall conclusion is that adhesion strength can significantly be increased by controlling the particle in-flight properties. It should be remarked that external cooling was not included in this latter analysis. As previously shown, this parameter has a significant

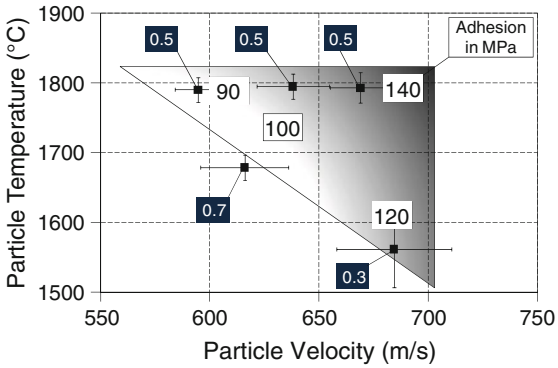

Fig. 6 Particle in-flight properties—adhesion strength process map

influence on coating adhesion strength. Microstructure evaluations were finally performed to better understand the fundamental reasons for this relationship.

3.3 Relationships Between Microstructure Properties and Adhesion Strength

A metallographic investigation was performed for all experimental runs (Fig. 7). Porosity and oxides content were quantified by image analysis algorithm through 60 optical micrographs (200×) for each run. The relationships between porosity/oxides content and particle in-flight characteristics on one hand, and coating adhesion strength on the other, could be well described by the derived MLR model (Table 3). Coefficients of linear regression (R2) have to be considered as very high for both porosity and oxide contents using a confidence level of 0.95. Contour plots based on derived MLR model are shown in Fig. 8. Lower porosity (Fig. 8a) and higher oxides content (Fig. 8b) were observed when increasing the particle velocity, whereas an increase in particle temperature in the studied range had a smaller effect on porosity, and no significant effect on oxides content. The increase of the in-flight oxidation with the particle velocity might be explained by the increase of the free oxygen partial pressure (Ref 7): while processing at a higher total mass flow, higher turbulences lead to entrapped air in the plume and thus more oxygen (Ref 8). Eventually from such a statistical approach, the increase in coating adhesion strength is attributed to a significant decrease in porosity (Fig. 8c).

It has to be noted that both porosity and oxides content were not significantly affected by the factor external cooling, compared to the coating adhesion strength (Fig. 8d). Even if the relationship between porosity/oxides content and adhesion strength seems possible to explain by the change in particle in-flight properties, there obviously has to be another explanation to the increase in coating adhesion strength when no external cooling is processed (Fig. 8d), thus explaining the low coefficient of linear regression for the adhesion strength response in the MLR model (Table 3). Runs N2 and N6 (Fig. 5) have

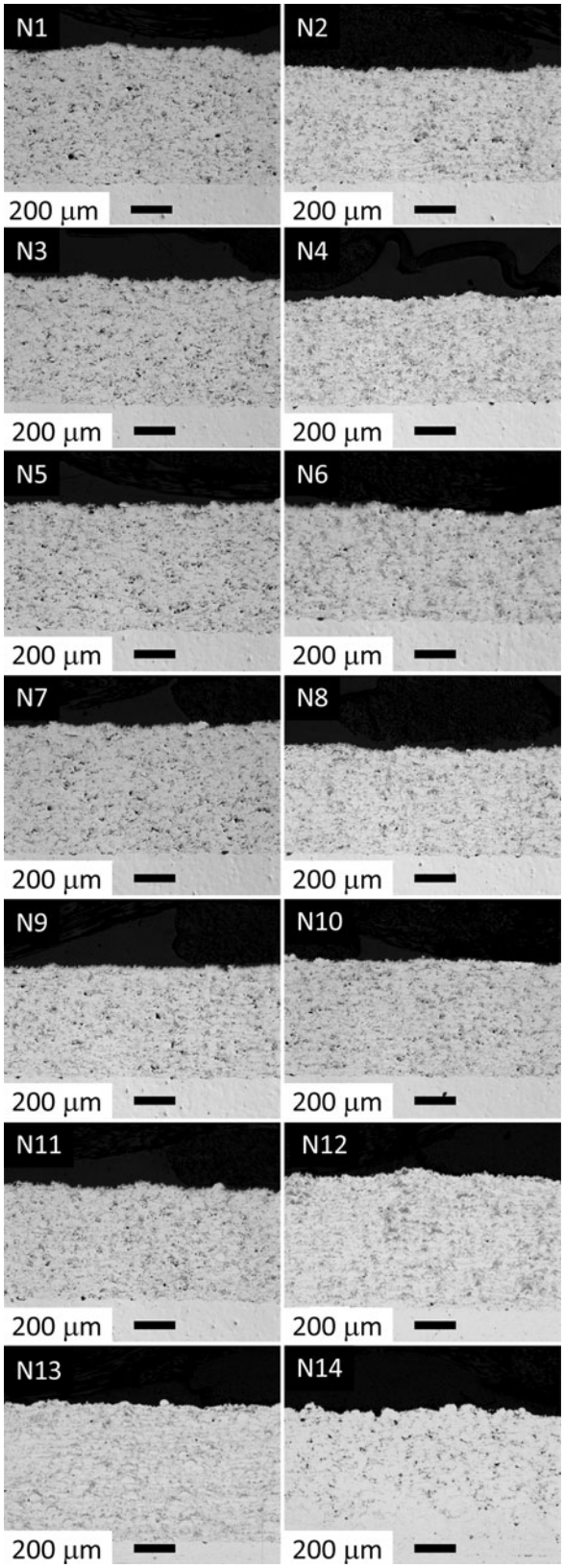

Fig. 7 Optical micrographs (50×) of cross section of sprayed samples from the design matrix (Table 1); runs from N1 to N11 participate to the derived MLR model

Table 3 Statistics from MLR regression models for particle in-flight diagnostics map

Coeff.	Adhesion strength	Porosity level	Oxides content
Runs	11	11	11
DF	7	7	7
R2	0.676	0.978	0.896
Q2	0.348	0.960	0.754
RSD	16.25	0.10	1.27
Conf.lev.	0.95	0.95	0.95

DF residual degree of freedom, *R2* coeff. linear regression, *Q2* coeff. prediction ability, *RSD* residual standard deviation

similar coating microstructure, equivalent particles temperatures and equivalent (high) particles velocities, but significantly different adhesion strengths, 148 ± 8 MPa and 110 ± 15 MPa, respectively. The difference between run N2 and run N6 was that in run N2 no external cooling was used. Since external cooling directly influences the cooling rate of deposited layers per pass, different levels of cooling stresses are generated. The redistribution of residual stresses through the coated system might be one explanation to the difference in coating adhesion strength (Ref 9). Such relationship between residual stress and coating adhesion has already been investigated in our previous study, when studying a possible effect of thickness on adhesion (Ref 9). Independently of the coating thickness, the coating adhesion was attributed to a stresses accommodation at the coating/substrate interface. When depositing thicker coatings, longer spraying sequence may promote a thermal relaxation of accumulated stresses through the system, which is part of a current investigation. To be able to fully model the effect of external cooling on coating adhesion, the residual stress level will be included in future work, as well as the substrate temperature during deposition (Ref 10). Such a model will enable adhesion strength to be maximized taking microstructure boundary conditions into account.

4. Summary and Conclusion

Relationships between process parameters, particle in-flight characteristics, coating microstructure properties and adhesion strength were developed in this study. The main results can be summarized as:

- The relationship between process parameters and coating adhesion strength was well explained by the particle in-flight properties.
- The relationships between particle in-flight properties and adhesion strength can be summarized as: the higher the particle velocity and the particle temperature, the higher the adhesion strength.
- A clear relationship between particle in-flight properties and coating microstructure was derived: the

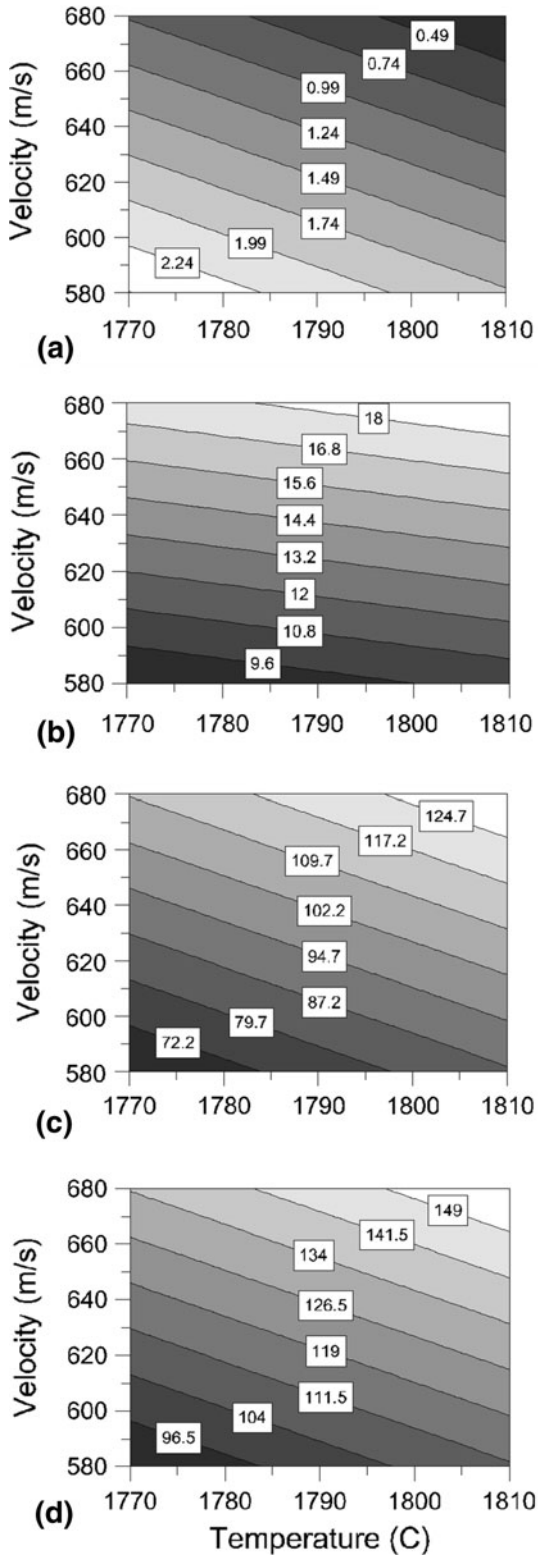

Fig. 8 Contour plots of (a) porosity (%), (b) oxide content (%) and coating adhesion (MPa) with (c) and without (d) cooling

higher the particle velocity, the lower the porosity level and higher the oxides content.

- Coating microstructure, i.e., porosity and oxides content, seems independent of external cooling treatment. However, coating adhesion strength is strongly dependent on substrate cooling.
- Investigations on the role of residual stresses on coating adhesion strength, as well as monitoring of the substrate temperature, might give further in-sight to the substrate cooling effect on adhesion strength. By including residual stresses in the model building relationships between process parameters, residual stresses, coating microstructure, and adhesion strength can be derived for both industrial optimization and academic purposes.

Acknowledgments

The authors acknowledge the financial support of the VINNOVA funded NFFP4 project and the technical support of the Thermal Spray Department at Volvo Aero Corporation (Trollhättan, Sweden). The authors would like to acknowledge J. Johansson (VAC) for the DPV2000 acquisitions, and H. Dahlin and M. Ottosson (University West) for their technical support in brazing experiments.

References

1. M. Watanabe, S. Kuroda, K. Yokoyama, T. Inoue, and Y. Gotoh, Modified Tensile Adhesion Test for Evaluation of Interfacial Toughness of HVOF Sprayed Coatings, *Surf. Coat. Technol.*, 2008, **202**, p 1746-1752
2. L. Pawlowski, *The Science and Engineering of Thermal Spray Coatings*, John Wiley & Sons, West Sussex, England, 1995
3. V.V. Sobolev, J.M. Guilemany, and J. Nutting, *High Velocity Oxy-Fuel Spraying: Theory, Structure-Property, Relationships and Applications*, Shrikant Joshi, Ed., Maney Publishing, London, 2004
4. ASTM C633-79, *Standard Method of Test for Adhesion or Cohesive Strength of Flame-Sprayed Coatings*, American Society for Testing and Materials, Philadelphia, 1982, p 636-642
5. ASTM E562-08, *Standard Test Method for Determining Volume Fraction by Systematic Point Count*, American Society for Testing and Materials, Philadelphia, 2008
6. C. Lyphout, P. Nylén, U. Klement, and M. Sattari, Characterization of Adhesion Strength of HVOF Sprayed IN718 Coatings, *Surf. Modif. Technol.*, 2008, **XXII**, p 11-18
7. H. Choi, S. Lee, B. Kim, H. Jo, and C. Lee, Effect of In-flight Particle Oxidation on the Phase Evolution of HVOF NiTiZrSiSn Bulk Amorphous Coating, *J. Mater. Sci.*, 2005, **40**, p 6120-6126
8. R. Molins, B. Normand, G. Rannou, B. Hannoyer, and H. Liao, Interlamellar Boundary Characterization in Ni-based Alloy Thermally Sprayed Coating, *Mater. Sci. Eng.*, 2003, **A351**, p 325-333
9. C. Lyphout, P. Nylén, A. Manescu, and T. Pirling, Residual Stresses Distribution through Thick HVOF Sprayed Inconel 718 Coatings, *J. Therm. Spray Technol.*, 2008, **17**(5-6), p 915-923
10. C. Moreau, Towards a Better Control of Thermal Spray Process, *Thermal Spray: Meeting the Challenges of the 21st Century*, C. Coddet, Ed., ASM International, Materials Park, OH, 1998, p 1681-1693